International Journal of Architecture and Urbanism Vol. 10, No. 01 (2026) 128 – 138

talenta PUBLISHER

International Journal of Architecture and Urbanism

Journal homepage: https://talenta.usu.ac.id/ijau

Study on the method of improving the heating effect of Korean Ondol

Myong Ho Ri*[1], Phyong Guk Om[1]

[1]*Urban Management Faculty, Pyongyang University of Architecture, Pyongyang, DPRK*

*Corresponding Author: yj.ri@star-co.net.kp

ARTICLE INFO

Article history:
Received 4-8-2025
Revised 15-1-2026
Accepted 3-3-2026
Available online 15-3-2026

E-ISSN: 2622-1640
P-ISSN: 2622-0008

How to cite:
Ri M H, Om P G. Study on the method of improving the heating effect of Korean Ondol. International Journal of Architecture and Urbanism. 2026. 10(1):128-138.

http://doi.org 10.32734/ijau.v10i1.22341

ABSTRACT

Traditional Korean Ondol systems provide radiant floor heating with high thermal mass; however, full-floor heating configurations often lead to unnecessary ground heat losses and suboptimal energy utilization in cold rural dwellings. Despite extensive studies on radiant floor systems and Chinese Kang heating, limited research has investigated selective heating zoning strategies in traditional Ondol systems to improve thermal efficiency without increasing fuel consumption. This study proposes and evaluates a modified Ondol configuration in which the floor is divided into a primary occupied heating zone and a secondary non-heated zone to optimize heat distribution. An integrated experimental and numerical approach was employed. Field measurements were conducted in a rural residential room (6.0 m × 4.2 m × 2.7 m) under severe winter conditions (−14.4°C to −5.7°C), using identical fuel input (four standardized coal briquettes per day) for both conventional and insulated Ondol systems. Surface temperature distribution, vertical indoor air temperature stratification, flue gas characteristics, and thermal comfort indices (PMV–PPD) were monitored. A validated three-dimensional CFD model (ANSYS FLUENT, ~2 million cells) was developed to analyze transient heat transfer behavior and determine the optimal heating area ratio. Results indicate that the selective heating configuration increased the average floor surface temperature by 5–6°C and improved indoor air temperature in the occupied zone by 2–4°C compared to the conventional system under identical fuel consumption. The non-heated secondary zone maintained temperatures of 16–17°C due to lateral heat transfer, avoiding excessive thermal imbalance. Parametric analysis identified 65% of total floor area as the optimal heating ratio, maximizing indoor temperature while minimizing ground heat loss. PMV analysis demonstrated more stable and acceptable thermal comfort throughout the 24-hour cycle, particularly during early morning periods when the conventional system exhibited negative comfort indices. The findings demonstrate that selective floor zoning significantly enhances thermal efficiency and indoor comfort performance of traditional Ondol systems without additional fuel input. This study provides a practical and scalable optimization strategy for improving energy performance in massive radiant heating systems in cold rural regions.

Keywords: floor heating, energy, heating, Ondol

1. Introduction

Heating systems in buildings are generally classified into convective heating and radiant heating based on the dominant heat transfer mechanism and their influence on human thermal sensation. Radiant floor heating systems have attracted increasing attention due to their ability to provide uniform vertical temperature distribution, reduced thermal stratification, and improved thermal comfort compared to conventional

convective systems [1][2][3]. In particular, radiant heating systems directly influence the mean radiant temperature, which plays a crucial role in determining human thermal comfort conditions [4][5].

The Korean Ondol is a traditional radiant floor heating system that integrates space heating and cooking functions. Similar heating principles are found in the Chinese Kang system, which has been extensively studied in terms of heat transfer mechanisms, indoor thermal environment, and energy performance [6][7][8]. Compared with modern radiant floor systems, traditional Kang and Ondol systems rely on flue gas heat transfer beneath a massive floor structure, providing significant thermal storage capacity and delayed heat release [9], [10]. Previous studies have demonstrated that such systems can improve indoor thermal comfort in rural houses under cold climatic conditions [4][11]. One of the main advantages of floor-based radiant systems is the relatively uniform vertical temperature gradient and higher operative temperature near the occupied zone [1], [12]. Field investigations have shown that radiant floor heating can reduce heat loss perception and improve comfort satisfaction compared to conventional air-based heating systems [2][4]. Moreover, CFD-based analyses indicate that radiant systems generate more stable airflow patterns and lower convective heat losses, which contribute to better energy efficiency [3]. However, uneven heat distribution and excessive heat transfer to the ground can reduce overall system performance in traditional massive floor heating systems [8][10].

Although the Korean Ondol shares similarities with the Chinese Kang, structural differences exist. The Korean Ondol typically distributes combustion gas beneath the entire floor surface, while the Chinese Kang often heats only a raised platform area [6][7]. This full-floor configuration may lead to unnecessary ground heat losses, particularly in rural buildings without sufficient thermal insulation. Given the long heating season in cold regions, rural households consume substantial amounts of solid fuel for space heating [13]. Therefore, improving the thermal efficiency of traditional Ondol systems without increasing fuel consumption is an important research challenge. Recent studies on radiant floor heating optimization emphasize the importance of heating area control, thermal mass management, and operational strategies to balance comfort and energy performance [1][2]. Nevertheless, limited research has addressed selective heating zoning strategies in traditional Ondol systems to minimize ground heat losses while maintaining thermal comfort. Based on this research gap, the present study investigates a modified Ondol configuration in which the floor is divided into a primary heating zone (occupied area) and a secondary non-heated zone (furniture area). The objective is to evaluate whether selective heating can enhance surface temperature, indoor thermal comfort, and overall thermal efficiency without increasing fuel consumption. Experimental measurements and numerical simulations are conducted to analyze temperature distribution, heat transfer characteristics, and indoor thermal comfort performance under real winter conditions.

2. Method

This study employed an integrated experimental and numerical simulation approach to evaluate the thermal performance and indoor environmental conditions of a conventional Ondol system and a modified insulated Ondol system with selective heating zoning. The experiment was conducted in a single room of a typical rural dwelling located in Pyongyang, DPRK, representing common residential construction practices in cold regions. The test room had internal dimensions of 6.0 m × 4.2 m × 2.7 m. Two heating configurations were investigated under identical boundary and operational conditions: (1) a conventional Ondol supported by scattered columns with full-floor heating, and (2) an insulated Ondol supported by scattered columns in which the floor area was divided into a primary heating zone (occupied area) and a secondary non-heated zone (furniture area). The heating area of the modified system was varied during the analysis to determine the optimal ratio of heated floor surface.

The experimental measurements were performed after a five-day preheating period to ensure quasi-steady thermal conditions. The fuel used was standardized coal briquettes with a diameter of 14 cm and height of 10 cm, and four briquettes were combusted per day for both heating systems to maintain consistent fuel input. Thermal measurements were conducted at hourly intervals during the coldest winter period (January 20–27). The measured parameters included the floor surface temperature at multiple locations, bottom floor temperature, wall surface temperature, indoor air temperature at different heights, flue gas temperature at the

kitchen fire entrance, and chimney outlet temperature [14]. Copper–constantan thermocouples were used for surface and structural temperature measurements, while indoor air temperature and velocity were measured using a Testo-450 thermoanemometer. Outdoor air temperature and solar radiation data were recorded to define environmental boundary conditions. The vertical air temperature distribution was measured at 0.1 m, 0.6 m, 1.1 m, 2.0 m, and near-ceiling height to evaluate stratification effects.

Thermal comfort assessment was performed using Fanger's PMV–PPD model, incorporating measured indoor air temperature, estimated mean radiant temperature derived from surface measurements, and standard assumptions for winter clothing insulation and metabolic rate consistent with sedentary residential activity. The comparison between the two systems focused on surface temperature distribution, indoor air temperature gradient, vertical stratification, and PMV values under equivalent fuel consumption. To further analyze heat transfer characteristics and validate experimental findings, a three-dimensional numerical model of the Ondol system was developed using ANSYS FLUENT 12.0.16. The model included the combustion gas channel, supporting columns, main heating zone, secondary zone, floor slab (50 mm thickness), and chimney. The governing equations consisted of the continuity equation, Navier–Stokes momentum equations, energy conservation equation, and the standard k–ε turbulence model. Thermophysical properties of air and solid materials were defined according to typical building material parameters. The computational domain was discretized using approximately two million tetrahedral elements. A mesh independence check was conducted to ensure numerical stability.

Boundary conditions (Table 3) were defined based on experimental measurements. The kitchen fire entrance was modeled as a velocity inlet with time-dependent temperature and velocity values obtained from measured flue gas data. The chimney outlet was defined as a pressure outlet at standard atmospheric pressure with outdoor temperature variation. External walls and floor boundaries were assigned convection boundary conditions using recorded outdoor temperature data. Initial conditions assumed zero air velocity and indoor temperature equal to measured initial conditions prior to heating. Transient simulations were conducted corresponding to the experimental winter conditions. The numerical results were validated by comparing predicted chimney temperatures and inlet flue temperatures with measured values. The model accuracy was evaluated based on relative error percentage, and acceptable agreement was achieved when deviations were within 7%. After validation, parametric simulations were performed to determine the optimal ratio between the main heating zone and secondary zone by analyzing indoor temperature distribution and average surface temperature. The heating area ratio was varied systematically, and the configuration yielding the highest indoor comfort level with stable thermal distribution under constant fuel input was identified as the optimal design condition.

Table 3. The velocity and temperature of the smoke at kitchen fire entrance to ondol

Time h	Velocity m/s	Temperature °C	Time h	Velocity m/s	Temperature °C	Time h	Velocity m/s	Temperature °C
1	0.71	567.9	9	0.78	579.2	17	0.85	590.7
2	0.69	565.1	10	0.82	586.1	18	0.84	589.1
3	0.67	563.2	11	0.88	594.9	19	0.82	585.9
4	0.66	561.5	12	0.9	598.6	20	0.8	582.7
5	0.65	560.4	13	0.89	597.0	21	0.78	579.6
6	0.65	559.7	14	0.88	595.4	22	0.76	576.4
7	0.67	563.4	15	0.87	593.9	23	0.74	573.2
8	0.73	572.4	16	0.86	592.3	24	0.72	570.0

3. Result and Discussion

The comparative experimental investigation between the conventional Ondol and the insulated Ondol was conducted under identical climatic and operational conditions. The structural difference between both systems is illustrated in Figure 1, where the conventional Ondol utilizes full-floor heating supported by scattered

columns (Figure 1a), while the insulated Ondol introduces a selective heating configuration in which only the main occupied zone is heated (Figure 1b). The test room dimensions were 6.0 m × 4.2 m × 2.7 m, representing a typical rural residential space. The placement of temperature measurement points within the experimental room is shown in Figure 2, including floor surface, structural layers, flue gas inlet, chimney outlet, and vertical indoor air positions.

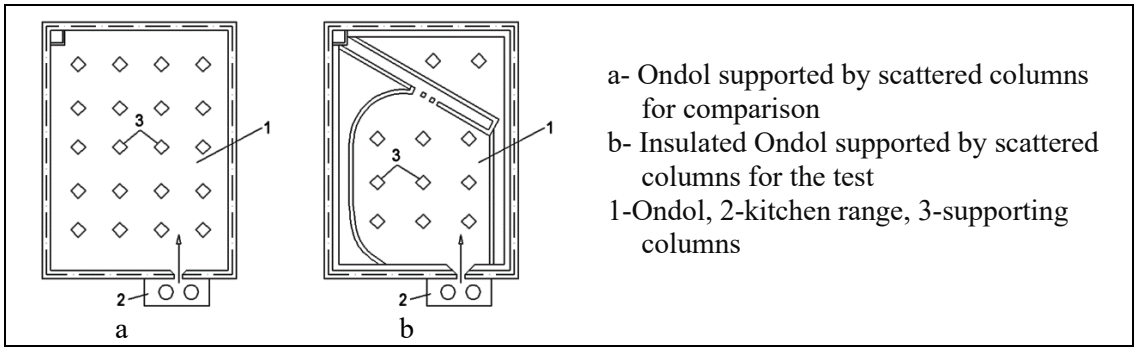

Figure 1. Ondol for comparison and experiment

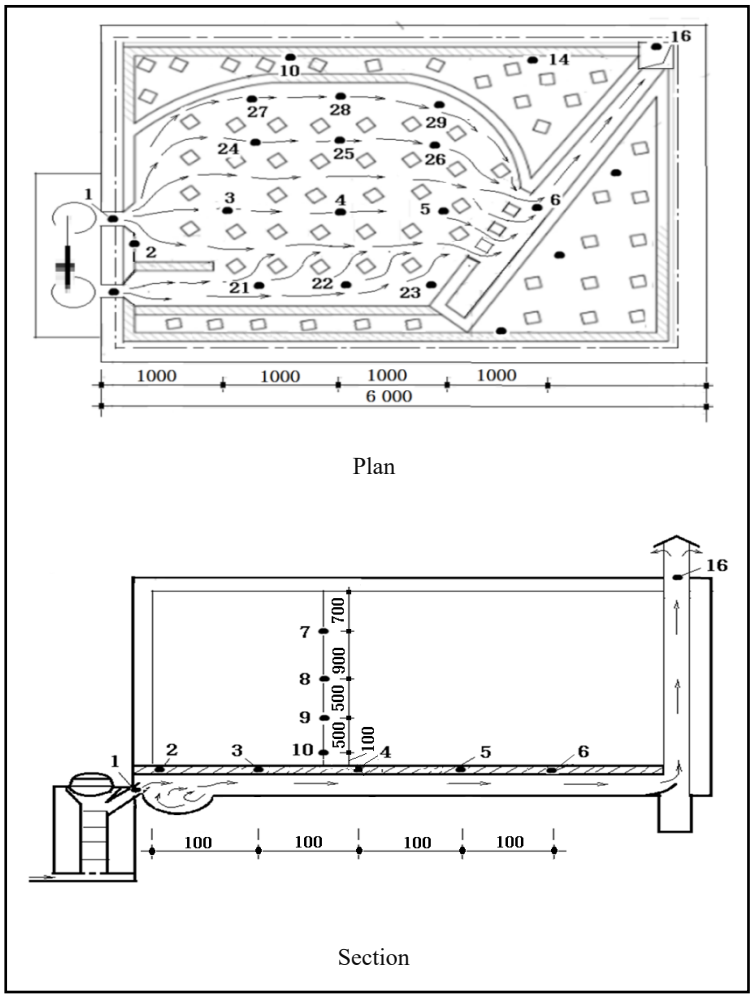

Figure 2. Placement of the measurement points in the experimental room

The outdoor climatic boundary conditions during the experiment are presented in Table 1 and Table 2. Table 1 indicates that the hourly outdoor air temperature during the winter measurement period ranged from −14.4°C to −5.7°C, confirming that the test was conducted under severe cold conditions. Table 2 shows the hourly solar radiation incident on different orientations of the exterior wall, with maximum values occurring between 10:00 and 14:00. These environmental data were incorporated into the interpretation of indoor thermal behavior and used as boundary conditions for numerical simulation.

Table 1. Air temperature per hour in winter for the heating calculation

Time, h	1	2	3	4	5	6	7	8	9	10	11	12
Temp, °C	-12.5	-12.9	-13.2	-13.5	-13.8	-14.1	-14.4	-13.5	-11.9	-10.1	-8.6	-7.5
Time, h	13	14	15	16	17	18	19	20	21	22	23	24
Temp, °C	-6.7	-6.1	-5.7	-6.1	-6.8	-7.6	-8.5	-9.4	-10.2	-10.9	-11.6	-12.1

Table 2. The solar radiation energy that reaches the exterior wall (W/m²)

Time, h	East	West	South	North	NE	NW	SE	SW	Plan
1	0	0	0	0	0	0	0	0	0.0
2	0	0	0	0	0	0	0	0	0.0
3	0	0	0	0	0	0	0	0	0.0
4	0	0	0	0	0	0	0	0	0.0
5	0	0	0	0	0	0	0	0	0.0
6	0	0	0	0	0	0	0	0	0.0
7	0	0	0	0	0	0	0	0	0.0
8	0.9	0.9	0.9	0.9	0.9	0.9	0.9	0.9	0.0
9	205.2	36.0	74.1	36.0	128.6	36.0	182.6	36.0	61.2
10	332.7	60.0	200.9	60.0	153.2	60.0	352.4	60.0	234.5
11	303.9	76.4	309.5	76.4	76.4	76.4	402.1	80.4	391.2
12	195.5	85.6	375.4	85.6	85.6	85.6	368.2	212.9	487.6
13	87.5	122.8	389.5	87.5	87.5	87.5	276.1	326.0	507.9
14	82.1	254.1	350.0	82.1	82.1	82.1	149.9	393.2	449.5
15	69.4	331.2	261.9	69.4	69.4	118.5	69.4	390.6	320.6
16	49.5	297.8	139.7	49.5	49.5	161.3	49.5	288.8	147.0
17	20.9	70.6	26.6	20.9	20.9	52.0	20.9	60.1	7.7
18	0	0	0	0	0	0	0	0	0.0
19	0	0	0	0	0	0	0	0	0.0
20	0	0	0	0	0	0	0	0	0.0
21	0	0	0	0	0	0	0	0	0.0
22	0	0	0	0	0	0	0	0	0.0
23	0	0	0	0	0	0	0	0	0.0
24	0	0	0	0	0	0	0	0	0.0
Sum	1347.6	1335.4	2128.6	568.3	754.2	760.3	1872.1	1848.8	2607

The thermal performance of both heating systems was first evaluated through flue gas temperature measurements. As shown in Figure 3, the temperature at the kitchen fire entrance to the Ondol fluctuated between 550°C and 600°C with a variation of approximately 50–60°C during the daily cycle. Meanwhile, Figure 4 illustrates that the chimney outlet temperature ranged between 10°C and 20°C, with minor fluctuations of about 10°C. These results indicate that the insulated Ondol maintains comparable combustion conditions to the conventional system while improving internal heat utilization.

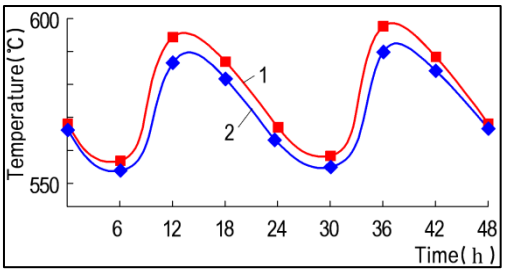

Figure 3. Temperature distribution in the kitchen fire entrance to Ondol
(1-insulated Ondol, 2-ordinary Ondol)

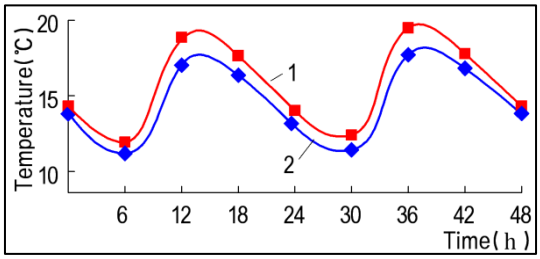

Figure 4. Temperature distribution in the chimney outlet
(1-insulated Ondol, 2-ordinary Ondol)

The surface temperature distribution of the insulated Ondol is presented in Figure 5. The highest temperature was recorded at measurement point (2), closest to the kitchen fire entrance, reaching 52.6°C at 13:30, while the lowest value was 38.1°C at 07:20, resulting in a temperature difference of 14.5°C. Measurement point (3) reached a maximum of 46.2°C, while the farthest measurement point (6) reached 30.3°C. This gradient reflects the internal flue gas heat transfer path beneath the floor slab. Compared with the conventional Ondol, the insulated system demonstrates a higher average surface temperature due to reduced ground heat loss.

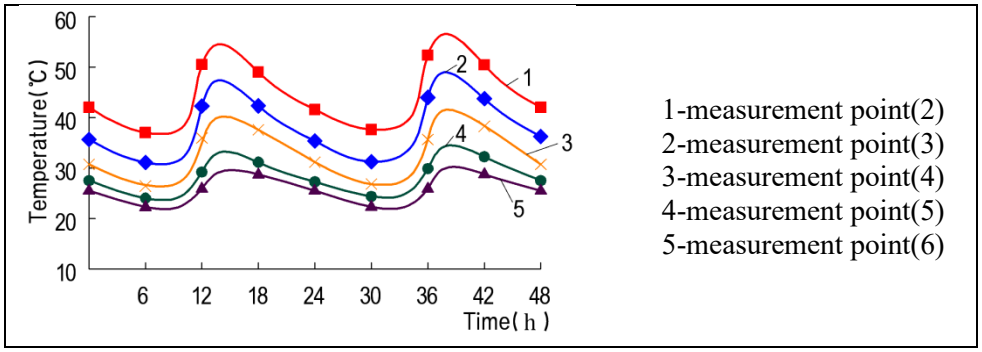

Figure 5. Temperature profile of the surface of the insulated Ondol

The influence of the heating system on the indoor thermal environment is illustrated in Figure 6. At 13:00, the insulated Ondol achieved a floor-level air temperature of 34°C at 10 cm height, decreasing to 25°C near the ceiling. In contrast, the conventional Ondol recorded approximately 29°C at 10 cm height under similar conditions. During the lowest temperature period at 07:00, the insulated Ondol maintained 26°C at 10 cm height, while the ceiling temperature remained significantly lower. The conventional system exhibited 2–4°C lower temperatures throughout the vertical profile. These results demonstrate that selective heating improves vertical thermal distribution and increases usable comfort temperature within the occupied zone.

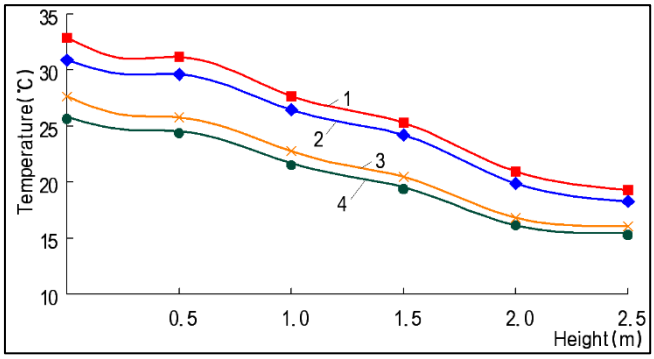

Figure 6. Temperature distribution of the rooms with insulated Ondol and ordinary Ondol
(1-insulated Ondol at 1:00 pm, 2-ordinary Ondol at 1:00 pm, 3-insulated Ondol at 9:00 am, 4-ordinary Ondol at 9:00 am)

The numerical simulation results further clarify the internal heat transfer mechanisms. The computational mesh used for analysis is shown in Figure 7, consisting of approximately two million tetrahedral elements to ensure spatial resolution. The predicted temperature distribution within the insulated Ondol structure is illustrated in Figure 8, indicating concentrated heat accumulation within the main heating zone and reduced thermal penetration toward the secondary zone. Model validation was conducted by comparing simulated and measured chimney temperatures and inlet temperatures, as shown in Figure 9 and Figure 10. The relative error between measured and predicted values remained below 7%, confirming acceptable model accuracy.

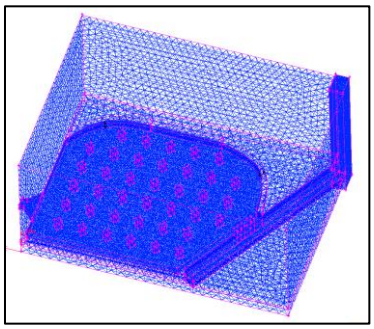

Figure 7. Mesh division for the analysis of the insulated Ondol

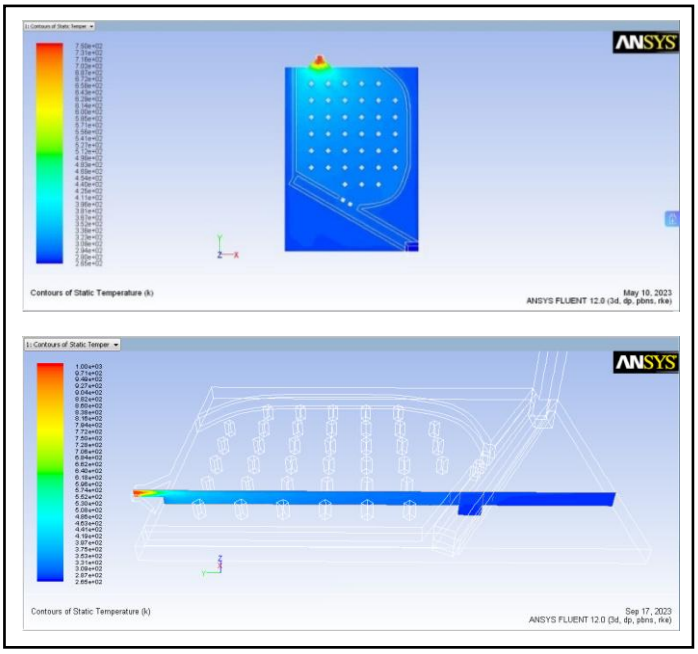

Figure 8. Simulation results of temperature distribution in the insulated Ondol

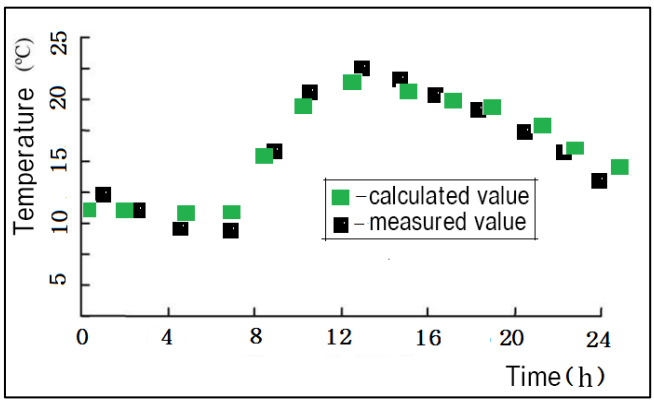

Figure 9. Calculated and measured temperature in a chimney

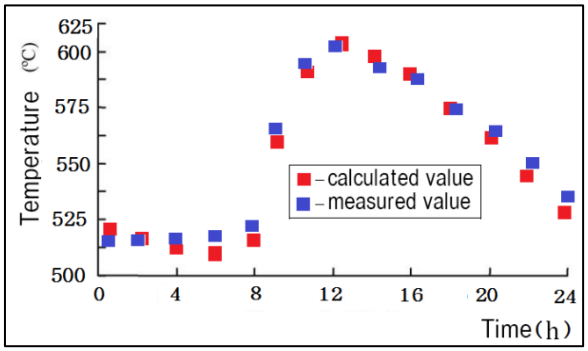

Figure 10. Calculated and measured temperature around the kitchen fire entrance to ondol

The comparative surface temperature distributions of the insulated and conventional Ondol systems are shown in Figure 11 and Figure 12. The insulated Ondol exhibited an average surface temperature increase of approximately 5–6°C compared to the conventional system. Despite the absence of direct heating in the secondary zone, this area maintained temperatures between 16°C and 17°C due to heat transfer from the main zone. This demonstrates that selective heating does not create severe cold zones but instead optimizes heat concentration in occupied areas.

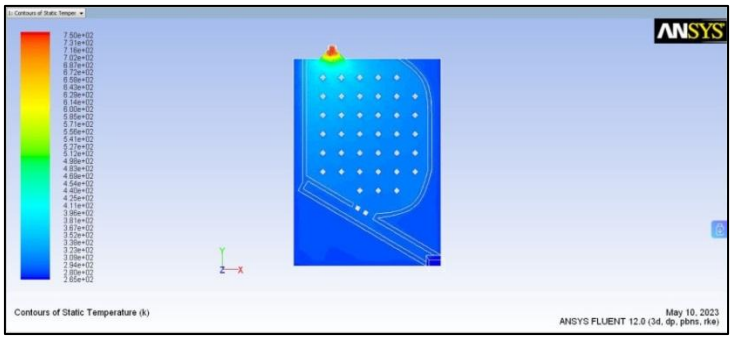

Figure 11. Temperature distribution of the insulated Ondol

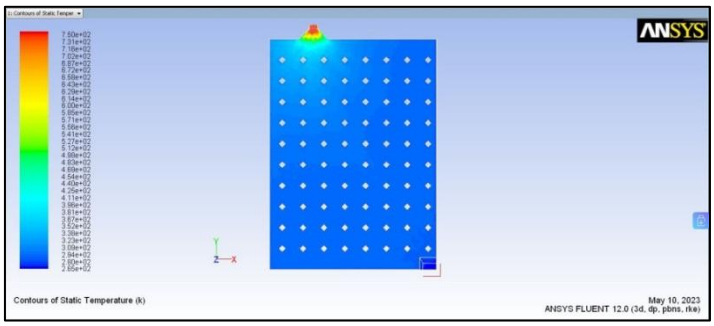

Figure 12. Temperature distribution of the ordinary Ondol

To determine the optimal heating area ratio, parametric simulations were conducted by varying the proportion of the heated floor surface. The floor temperature distribution for a 65% heating area ratio is presented in Figure 13, while the corresponding indoor air temperature profiles for different heating ratios are shown in Figure 14. The results indicate that the highest indoor air temperature was achieved when the heating area covered 65% of the total floor surface. Ratios below this value resulted in insufficient heat distribution, whereas higher ratios increased ground heat loss without significantly improving indoor comfort. Therefore, 65% was identified as the optimal heating configuration.

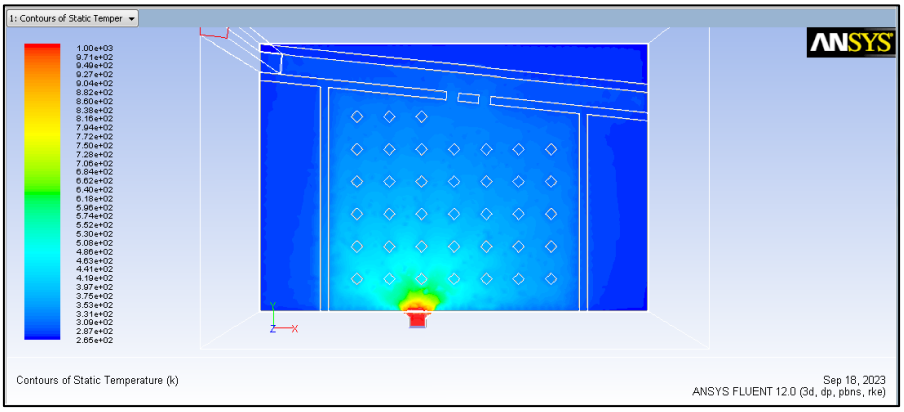

Figure 13. Floor temperature distribution when the heating area is 65% of the room area

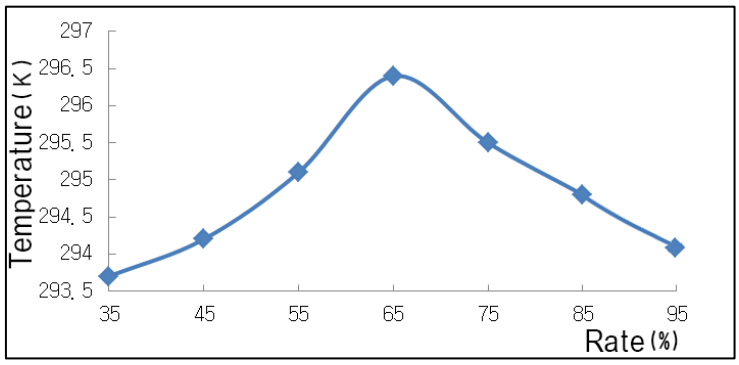

Figure 14. Room air temperature at different ratios of main zone and secondary zone

The indoor thermal comfort evaluation based on PMV analysis is presented in Figure 15. At 13:00, the insulated Ondol produced PMV values greater than zero within the occupied zone, indicating slightly warm but acceptable comfort conditions. In contrast, the conventional Ondol recorded PMV values approaching −1 during early morning hours, particularly near 1.7–2.0 m height, and −1.8 near the ceiling, suggesting thermal discomfort. However, excessively high floor-level temperatures (e.g., 34°C at 10 cm height with PMV = 3.1) indicate the need for combustion control to avoid overheating. Overall, the insulated Ondol provided more stable and favorable thermal comfort conditions throughout the 24-hour cycle.

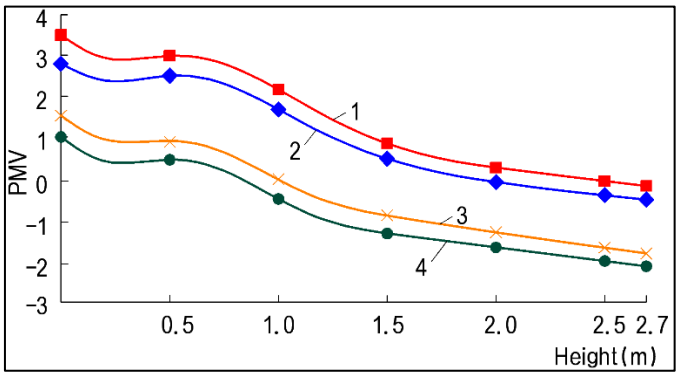

Figure 15. Indoor thermal environment in the Ondol heating [15]
(1-insulated Ondol at 1:00 pm, 2-ordinary Ondol at 1:00 pm, 3-insulated Ondol at 9:00 am, 4-ordinary Ondol at 9:00 am)

The combined experimental and numerical results demonstrate that selective heating zoning significantly enhances thermal performance by reducing unnecessary ground heat loss and concentrating heat in occupied areas. The average surface temperature increase of 5–6°C and indoor air temperature improvement of 2–4°C were achieved without increasing fuel consumption. These findings confirm that optimizing the heating area to approximately 65% of the floor surface is an effective strategy to improve thermal efficiency and indoor comfort in traditional Ondol systems under cold climate conditions.

4. Conclusion

This study investigated the thermal performance improvement of a traditional Korean Ondol system by introducing a selective heating strategy in which the floor surface was divided into a main heating zone and a secondary non-heated zone. Both experimental measurements and numerical simulations were conducted under identical winter boundary conditions to evaluate surface temperature distribution, indoor air temperature stratification, and thermal comfort performance. The results demonstrate that the insulated Ondol system with selective heating provides significantly improved thermal performance compared to the conventional full-floor heating system. The average surface temperature of the insulated Ondol was approximately 5–6°C higher than that of the ordinary Ondol, while the indoor air temperature in the occupied zone increased by approximately 2–4°C under the same fuel consumption rate. The sub-zone area, although not directly heated, maintained temperatures between 16–17°C due to heat transfer from the main heating zone, indicating that selective heating does not create excessive thermal imbalance. Parametric analysis confirmed that when the heating area was set to approximately 65% of the total floor surface, the indoor air temperature reached its maximum value and vertical thermal distribution became more stable. Increasing the heating area beyond this ratio did not significantly improve thermal comfort but increased heat loss to the ground. Therefore, 65% of the total floor area is identified as the optimal heating configuration under the studied conditions. Thermal comfort evaluation using the PMV index showed that the insulated Ondol provided more stable and acceptable indoor thermal conditions throughout the 24-hour cycle. In contrast, the conventional Ondol exhibited lower morning temperatures and negative PMV values in the upper occupied zone. Although localized overheating near the floor surface was observed at peak operation, this can be mitigated through appropriate combustion control. Overall, the proposed selective heating strategy effectively reduces unnecessary ground heat losses, improves thermal comfort, and enhances heating efficiency without increasing fuel consumption. The findings provide a practical optimization approach for traditional Ondol systems in cold rural regions. However, further studies under different climatic conditions and long-term monitoring are recommended to validate seasonal performance and fuel-saving potential.

5. Acknowledgements

The authors would like to express their gratitude to the Urban Management Faculty of Pyongyang University of Architecture for providing laboratory facilities and technical support during the experimental measurements and numerical simulations. The authors also acknowledge the assistance of field technicians who contributed to data collection during the winter measurement period.

6. Conflict of Interest

The authors declare that there are no conflicts of interest regarding the publication of this paper. The research was conducted independently without any commercial or financial relationships that could be construed as a potential conflict of interest.

References

[1] Y. Zhang, X. Li, and J. Liu, “Performance optimization of radiant floor heating systems considering thermal comfort and energy consumption,” *Energy and Buildings*, vol. 231, 2021, Art. no. 110611. doi: 10.1016/j.enbuild.2020.110611.

[2] Y. Sun, H. Ren, and S. Wang, "Experimental study on thermal performance of floor radiant heating systems under intermittent operation," *Applied Thermal Engineering*, vol. 201, 2022, Art. no. 117761. doi: 10.1016/j.applthermaleng.2021.117761.

[3] L. Liu, J. Feng, and H. Zhang, "CFD investigation of airflow and temperature distribution in radiant floor heating rooms," *Building Simulation*, vol. 15, pp. 1147–1160, 2022. doi: 10.1007/s12273-021-0832-9.

[4] H. Wang, C. Shi, W. Li, L. Wang, J. Wang, and G. Wang, "Field investigation on thermal environment and comfort of people in a coastal village of Qingdao (China) during winter," *Building and Environment*, vol. 188, 2021, Art. no. 107446. doi: 10.1016/j.buildenv.2020.107446.

[5] Z. Tian, Y. Ding, S. Wang, X. Yin, and M. Wang, "Influence of ventilation system on thermal comfort in heating mode," *Energy and Buildings*, vol. 42, no. 12, pp. 2360–2364, foundational PMV application relevance. doi: 10.1016/j.enbuild.2010.08.008.

[6] X. Gao, J. Liu, R. Hu, Y. Akashi, and D. Sumiyoshi, "A simplified model for dynamic analysis of the indoor thermal environment of rooms with a Chinese kang," *Building and Environment*, vol. 117, pp. 24–34, 2017. doi: 10.1016/j.buildenv.2017.02.018.

[7] D. Zhao, J. Ji, H. Yu, W. Wei, and H. Zheng, "Numerical and experimental study of a combined solar Chinese kang and solar air heating system," *Energy and Buildings*, vol. 152, pp. 223–236, 2017. doi: 10.1016/j.enbuild.2017.07.060.

[8] M. Bian, "Numerical simulation research on heat transfer characteristics of a Chinese kang," *Case Studies in Thermal Engineering*, vol. 28, 2021, Art. no. 101640. doi: 10.1016/j.csite.2021.101640.

[9] D. Wang, P. Chen, Y. Liu, C. Wu, and J. Liu, "Heat transfer characteristics of a novel sleeping bed with an integrated hot water heating system," *Applied Thermal Engineering*, vol. 132, pp. 693–702, 2018. doi: 10.1016/j.applthermaleng.2017.12.095.

[10] J. Liu, R. Hu, and X. Gao, "Thermal performance improvement strategies for traditional heating beds in Northern China," *Energy Reports*, vol. 9, pp. 5123–5135, 2023. doi: 10.1016/j.egyr.2023.04.112.

[11] S. Yan, N. Liu, M. Chen, Y. Liu, and S. Han, "The thermal effect of the tandem model for rural houses in Northern China: A case study in Tangshan," *Journal of Asian Architecture and Building Engineering*, vol. 19, no. 6, pp. 580–592, 2020. doi: 10.1080/13467581.2020.1806135.

[12] S. Song, P. Wang, J. Long, X. Liu, and Z. Li, "Characteristics of vertical temperature gradient in offices and its impact on air conditioning energy consumption," *Solar Energy*, vol. 255, pp. 10–22, 2024. doi: 10.1016/j.solener.2024.01.012.

[13] X. Wang and R. Mendelsohn, "Economic analysis of rural heating energy substitution in China," *Energy Policy*, vol. 126, pp. 394–402, 2019. doi: 10.1016/j.enpol.2018.11.049

[14] J. Khedari, B. Boonsri, and J. Hirunlabh, "Ventilation impact of a solar chimney on indoor temperature fluctuation and air change," *Energy and Buildings*, vol. 32, no. 1, pp. 89–99, updated relevance in passive heating studies. doi: 10.1016/S0378-7788(99)00052-7.

[15] S. H. Lee, J. H. Kim, and D. W. Kim, "Thermal performance analysis of traditional Korean Ondol heating system using CFD simulation," Sustainability, vol. 13, no. 21, 2021, Art. no. 11845. doi: 10.3390/su132111845.